SEQUENTIAL VERSUS SUPEREXCHANGE ELECTRON TRANSFER IN THE PHOTOSYNTHETIC REACTION CENTER

Yuming Hu and Shaul Mukamel
Chemistry Department
Rochester, New York 14627, USA

ABSTRACT. We present a novel expression for the complete electron transfer rate matrix in a three level system, which holds for an arbitrary value of the system free energies and reorganization energies. When the intermediate energy level is sufficiently high we recover the conventional superexchange rate. The relative contribution of the superexchange and the sequential mechanisms in the primary electron transfer process in the photosynthetic reaction center is discussed.

1. Introduction

The primary electron transfer process in the photosynthetic reaction center (RC) involves a transition from a photoexcited Bacteriochlorophyll dimer (P) to Bacteriopheophytin (H). In this process the electron transfers over a distance of 17Å in 2.8 psec. Since a direct (through space) coupling between P and H is excluded by their large separation, it has been suggested that the Bacteriochlorophyll monomer (B), which is located between P and H plays an active role in this event.[1-3]
This system can be described using the following adiabatic (Born-Oppenheimer) model Hamiltonian

$$H = \sum_{j=1}^{3} |j\rangle H_j\langle j| + V_{12}(|1\rangle\langle 2| + |2\rangle\langle 1|) + V_{23}(|2\rangle\langle 3| + |3\rangle\langle 2|). \quad (1)$$

State $|1\rangle$ is the optically excited chlorophyll dimer state (P*BH), state $|3\rangle$ is the charge transfer state observed after 2.8 psec (P^+BH^-) and state $|2\rangle$ is a possible intermediate state (P^+B^-H). $H_j(Q)$ denotes the adiabatic Hamiltonian of the polar medium whose degrees of freedom are denoted collectively by Q. V_{jn} represents the electronic coupling between states $|n\rangle$ and $|j\rangle$. The direct coupling V_{13} between states $|1\rangle$ and $|3\rangle$ was neglected in Eq.(1). The complete kinetic scheme for this system involves a 3 x 3 rate matrix whose matrix element K_{jn} denotes the transition rate from state $|n\rangle$ to state $|j\rangle$; n,j = 1,2,3. There are two basic mechanisms that have been suggested for the electron transfer process.[2,3] The first is superexchange, whereby $|2\rangle$ serves as an intermediate virtual state. In the superexchange mechanism[2-4] level $|2\rangle$ is never populated and the electron tunnels from level $|1\rangle$ to $|3\rangle$. Level $|2\rangle$ simply contributes to the tunneling matrix element. The other possible mechanism involves a sequential process whereby the electron transfers from level

J. Jortner and B. Pullman (eds.), Perspectives in Photosynthesis, 171–184.

|1> to |2> and then from |2> to |3>. This mechanism is described by the rates K_{21} and K_{32} and does not involve K_{31}. Since in the sequential mechanism level |2> is intermediate in the kinetic scheme |1>→|2>→|3> and it could be populated in the course of the reaction. Ultrafast optical measurements[5] have shown that the rate of appearance of level |3> following the preparation of level |1> by photoexcitation is 3.6×10^{11} sec^{-1}. These measurements have failed to detect a transient population of level |2>. This observation could support the superexchange mechanism. However, a sequential scheme with $K_{32}/K_{21} \geq 70$ will be consistent with this as well.[6] Extensive additional linear and nonlinear spectroscopic information (such as hole-burning and photon echo) is available in this system.[7,8] A major obstacle in resolving this issue is the lack of precise information regarding many of the relevant energetic parameters.[2,3,9] In particular the vertical transition energy $\Delta G^0_{12} - \lambda_{12}$ is not known. ΔG^0_{12} is the free energy difference between states |1> and |2>, λ_{12} is the corresponding reorganization energy (Figure 1). The common superexchange expression is valid only when $\Delta G^0_{12} - \lambda_{12}$ is large enough and it diverges when $\Delta G^0_{12} - \lambda_{12} = 0$. In this paper we report a microscopic calculation of the rate matrix K_{jn} which is obtained by formulating the problem using the density matrix in Liouville space.[10] This formulation was applied earlier to nonadiabatic and adiabatic electron transfer in a two level system and was used to explore the role of the dynamics of solvation in electron transfer processes.[11] The present formulation provides a general connection between the dynamics of electron transfer and nonlinear optical processes such as four wave mixing.[12] We have shown that the interplay between the sequential and the superexchange mechanisms is completely analogous to the interplay between the Fluorescence and the Raman components in an optical measurement. This profound connection is apparent when the problem is formulated using the density matrix in Liouville space. Our expression is valid for any value of $\Delta G^0_{12} - \lambda_{12}$ and can therefore be used to explore the relative contribution of the superexchange and the sequential electron transfer even when all three levels are degenerate.

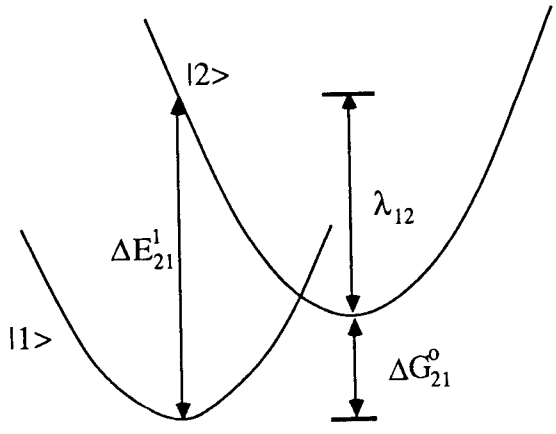

Figure 1: Configuration coordinate scheme showing the transition free energy ΔG^0_{21} the reorganization energy λ_{12} and the vertical transition energy ΔE^1_{21}. Similar schemes apply for the other pairs of levels (13 and 23).

2. Sequential and Superexchange Electron Transfer

We start our analysis by partitioning the nuclear Hamiltonian $H_j(Q)$ into the following terms

$$H_j(Q) = E_j + H_B + U_j \tag{2}$$

where E_j represents the electronic energy of the unsolvated state $|j\rangle$ and H_B represents the Hamiltonian of the bath, i.e. the nuclei of the RC which form a polar medium. U_j denotes the interaction between the electronic system and the medium, which may be expressed in terms of the polarization of the bath $P(\underset{\sim}{r})$, and the electrostatic field $D_j(\underset{\sim}{r})$ produced by the charge distribution of the system in the $|j\rangle$ state, i.e.

$$U_j = -\int dr\ D_j(\underset{\sim}{r}) \cdot P(\underset{\sim}{r}). \tag{3}$$

It should be emphasized that U_j depends on a macroscopic number of polarization degrees of freedom $P(\underset{\sim}{r})$, which undergo complicated motions resulting from thermal fluctuations. The statistical properties of U_j contain all the relevant information for our problem. We shall model U_j as Gaussian random variables. This is a common assumption in electron transfer theories.[2,3,13] It has been recently verified by an extensive numerical simulation of outer sphere electron transfer in water.[14] Eqs.(1) - (3) constitute our basic model Hamiltonian for the RC and they can be used to evaluate the electron transfer rates. We shall now introduce the following equilibrium density matrices for the bath

$$\rho_j = \exp(-H_j/k_BT)/\mathrm{Tr}\ \exp(-H_j/k_BT) \qquad j=B,1,2,3 \tag{4}$$

where Tr denotes a trace over the bath degrees of freedom. ρ_B is the density matrix of the bath in the absence of the electron transfer system. ρ_1, ρ_2 and ρ_3 are the density matrices of the bath when the electron transfer system is in states 1, 2 and 3, respectively. For the sake of simplicity we assume that the energy fluctuation U_j of the $|j\rangle$ state is totally uncorrelated with the energy fluctuation U_n on any other state $|n\rangle$, i.e.

$$\mathrm{Tr}\ (U_j\ U_n\ \rho_B) = 0 \qquad j \neq n \tag{5}$$

This is a reasonable assumption for the RC electron transfer, because the different electronic states correspond to the electron residing on different parts of RC, which have a different local environment, and their energy fluctuations are expected to be uncorrelated. The present calculation of the rate is based on formulating the dynamics in terms of the density matrix in Liouville space.[11] The formalism allows a perturbative expansion of the rate matrix K_{jn} in a power series in the nonadiabatic coupling V. This formalism was developed for electron transfer in a two level system resulting in general expressions for K_{21} and K_{32}.[11] We have extended the calculation to a three level system.[10] The calculation is based on expanding the rate matrix to fourth order V, followed by a partial resummation of the series to infinite order via a Pade approximant. It should be noted that the lowest order contribution to K_{21} and K_{32} is second order whereas for K_{31} it is fourth order. The bookkeeping of the various contributions is best illustrated using a Liouville-space coupling diagram. In Figure 2a we show the eight Liouville-space pathways contributing to K_{21} and in Figure 2b we show the three pathways contributing to K_{31}.

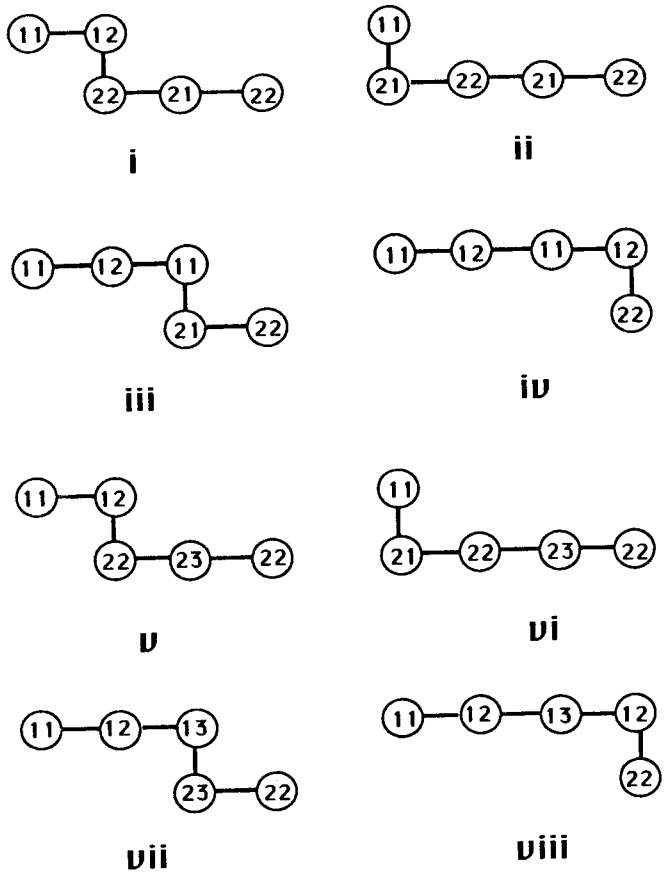

Figure 2a: The Liouville-space pathways[11] contributing to the rate K_{21} to fourth order in the nonadiabatic coupling. Each pair of indexes jn implies that the system is in the state |j><nl, where j=n stands for a population and j≠n for a coherence. Each bond represents a nonadiabatic coupling V. There are sixteen pathways which can lead from 11 to 22 in fourth order (four bonds). These pathways come in complex conjugate pairs so that we need consider only the eight pathways shown. Pathways (i) - (vi) represent a sequential nonequilibrium process whereby the system passes through an intermediate population. Pathways (vii) and (viii) represent a tunneling process.

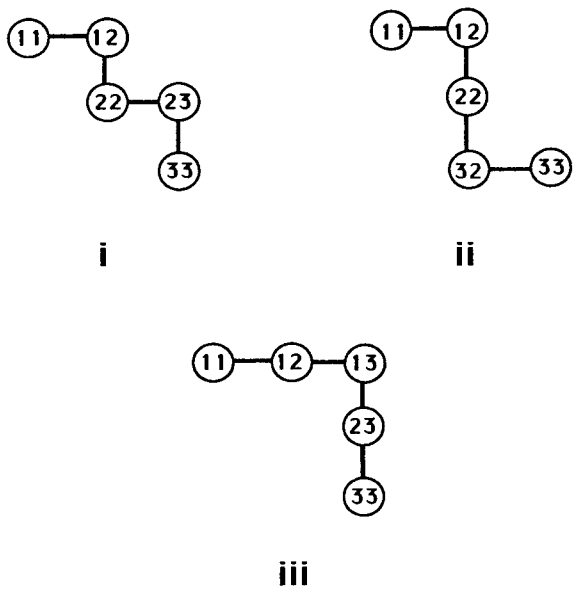

Figure 2b: The Liouville space pathways[11] contributing to the rate K_{31} to fourth order in the nonadiabatic coupling. There are six pathways which lead from 11 to 33 in fourth order. We need to consider only the three pathways shown (the others are their complex conjugates). Pathways (i) and (ii) represent a sequential nonequilibrium process and pathway (iii) is the tunneling (superexchange) term.

The rate matrix is given in terms of several physical quantities. We first define the free energy change for the |j> to |n> transition (Figure 1)

$$\Delta G^0_{jn} = \mathrm{Tr}(H_j\rho_j) - \mathrm{Tr}(H_n\rho_n), \tag{6}$$

and the vertical transition energy for this transition when the system is in state |m>

$$\Delta E^m_{jn} \equiv \mathrm{Tr}[(H_j - H_n)\,\rho_m]. \tag{7}$$

We further define the solvent reorganization energy in the |j> state

$$\lambda_j \equiv \mathrm{Tr}\,(U_j^2\,\rho_B)/2k_BT \tag{8}$$

and the reorganization energy for the |j> to |n> transition

$$\lambda_{jn} \equiv \lambda_j + \lambda_n\,. \tag{9}$$

Note that $\Delta E^m_{jn} = -\Delta E^m_{nj}$, $\Delta G^0_{jn} = -\Delta G^0_{nj}$ and $\lambda_{jn} = \lambda_{nj}$.

We next introduce the solvent correlation function

$$M_{jk}(t) = \frac{\langle \exp(i H_B t)\, U_{jk} \exp(-i H_B t)\, U_{jk}\, \rho_B \rangle}{\langle U_{jk}^2\, \rho_B \rangle} \tag{10a}$$

$$M(t) = \frac{\langle \exp(i H_B t)\, U_{23} \exp(-i H_B t)\, U_{12}\, \rho_B \rangle}{\sqrt{\langle U_{23}^2\, \rho_B \rangle \langle U_{12}^2\, \rho_B \rangle}}. \tag{10b}$$

The rate matrix was calculated by assuming a Gaussian statistics for U_j and using condition (Eq.(5)). The details of these calculations are given elsewhere.[10] We thus have

$$K_{21} = \frac{\sigma_{21}}{1+\sigma_{12}\tau_a+\sigma_{21}\tau_b+\sigma_{32}\tau_c} + \frac{2\pi}{\hbar} V_{12}^2 V_{23}^2 [R_{12} I(\eta_{12}^1) S_{12}(\Delta E_{12}^1) + R_{23} I(\eta_{23}^1) S_{23}(\Delta E_{23}^1)] \tag{11a}$$

$$K_{12} = \frac{\sigma_{12}}{1+\sigma_{12}\tau_a+\sigma_{21}\tau_b+\sigma_{32}\tau_c} + \frac{2\pi}{\hbar} V_{12}^2 V_{23}^2 [R_{12} I(\eta_{12}^2) S_{12}(\Delta E_{12}^2) + R_{23} I(\eta_{23}^2) S_{23}(\Delta E_{23}^2)] \tag{11b}$$

$$K_{32} = \frac{\sigma_{32}}{1+\sigma_{32}\tau_a'+\sigma_{23}\tau_b'+\sigma_{12}\tau_c} + \frac{2\pi}{\hbar} V_{12}^2 V_{23}^2 [R_{12} I(\eta_{12}^2) S_{12}(\Delta E_{12}^2) + R_{23} I(\eta_{23}^2) S_{23}(\Delta E_{23}^2)] \tag{11c}$$

$$K_{23} = \frac{\sigma_{23}}{1+\sigma_{32}\tau_a'+\sigma_{23}\tau_b'+\sigma_{12}\tau_c} + \frac{2\pi}{\hbar} V_{12}^2 V_{23}^2 [R_{12} I(\eta_{12}^3) S_{12}(\Delta E_{12}^3) + R_{23} I(\eta_{23}^3) S_{23}(\Delta E_{23}^3)] \tag{11d}$$

$$K_{31} = \sigma_{21}\sigma_{32}\tau_c + \frac{2\pi}{\hbar} V_{12}^2 V_{23}^2 [R_{13} I(\eta_{13}^1) S_{13}(\Delta E_{13}^1) - R_{12} I(\eta_{12}^1) S_{12}(\Delta E_{12}^1) - R_{23} I(\eta_{23}^1) S_{23}(\Delta E_{23}^1)] \tag{11e}$$

$$K_{13} = \sigma_{23}\sigma_{12}\tau_c + \frac{2\pi}{\hbar} V_{12}^2 V_{23}^2 [R_{13} I(\eta_{13}^3) S_{13}(\Delta E_{13}^3) - R_{12} I(\eta_{12}^3) S_{12}(\Delta E_{12}^3) - R_{23} I(\eta_{23}^3) S_{23}(\Delta E_{23}^3)] \tag{11f}$$

The diagonal elements of the rate matrix are given by

$$\begin{aligned} -K_{11} &= K_{21} + K_{31} \\ -K_{22} &= K_{12} + K_{32} \\ -K_{33} &= K_{13} + K_{23} \end{aligned} \tag{12}$$

σ_{jn} is the nonadiabatic transition rate from state n to j,

$$\sigma_{jn} \equiv \frac{2\pi}{\hbar} V_{jn}^2 S_{jn}(\Delta E_{jn}^n) \tag{13a}$$

where S_{jn} is the Franck Condon weighted density of states

$$S_{jn}(x) = \frac{1}{\sqrt{4\pi k_B T \lambda_{jn}}} \exp[-\frac{x^2}{4k_B T \lambda_{jn}}]. \tag{13b}$$

τ_j where j = a, b, c, a', b' are characteristic solvation timescales. They are defined as follows. We first introduce two timescale functions

$$\tau_{jk}(q) = \int_0^\infty dt \left\{ \frac{1}{\sqrt{1-M_{jk}^2(t)}} \exp[\frac{2M_{jk}(t)q^2}{1+M_{jk}(t)}] - 1 \right\} \tag{14a}$$

$$\tau(q,q') = \int_0^\infty dt \left\{ \frac{1}{\sqrt{1-M^2(t)}} \exp[\frac{2qq'M(t)-(q^2+q'^2)M^2(t)}{1-M^2(t)}] - 1 \right\}. \tag{14b}$$

Here q and q' are dimensionless parameters. We further define

$$q_{nm} \equiv \frac{\Delta E_{nm}^m}{\sqrt{4k_B T \lambda_{nm}}}. \tag{15}$$

In terms of these quantities we have $\tau_a = \tau_{12}(q_{12})$, $\tau_b = \tau_{12}(q_{21})$, $\tau_a' = \tau_{23}(q_{32})$, $\tau_b' = \tau_{23}(q_{23})$, $\tau_c = \tau(q_{32},q_{12})$. Note that $q_{nm} \neq q_{mn}$ and that τ_a and τ_b are obtained from τ_a and τ_b, respectively by interchanging the indexes 1 and 3. $\tau_{jk}(q)$ was calculated and analyzed previously in detail.[11] We further have

$$\Delta E_{nm}^n = \Delta G_{nm}^0 - \lambda_{nm} \tag{16a}$$

$$\Delta E_{nm}^m = \Delta G_{nm}^0 + \lambda_{nm} \tag{16b}$$

$$\Delta E_{nm}^k = \Delta G_{nm}^0 + \lambda_n - \lambda_m \qquad k \neq n,m \tag{16c}$$

$$\eta_{jn}^k = \sqrt{R_{jn}} \frac{\Delta E_{jm}^k \lambda_n + \Delta E_{nm}^k \lambda_j}{\lambda_{jn}} \tag{17}$$

$$R_{nm} = \frac{\lambda_{nm}}{[\lambda_1\lambda_2 + \lambda_1\lambda_3 + \lambda_2\lambda_3]\, 2k_B T} \tag{18}$$

where j, n, m are permutations of 1, 2, 3 and k = 1, 2, 3.
The function I(x) is given by

$$I(x) = -\int_0^\infty t \cos(x\,t) \exp(-t^2/2)\, dt\,. \tag{19}$$

I(x) is displayed in Figure 3. We have constructed the following Pade approximant for I(x),

$$I(x) \cong \begin{cases} \dfrac{-1 + 0.5851x^2}{1 + 0.4149x^2 + 0.1235x^4} & |x|<2.1 \\ \dfrac{-1 + 0.5994x^2}{11.2551 - 3.8396x^2 + 0.5994x^4} & |x|\geq 2.1 \end{cases} \tag{20}$$

The dashed line in Figure 3 shows the Pade approximant. The fit is excellent. We further note the following limiting behavior of I(x)

$$I(x) = \begin{cases} \dfrac{1}{x^2} & x >> 1 \\ -1 + x^2 & x << 1 \end{cases}. \tag{21}$$

3. Discussion

We shall now analyze our rate matrix (Eqs.(11)). We first note that to second order in V, Eqs.(11) reduce to the well known nonadiabatic rates[2,3] $K_{21} = \sigma_{21}$, $K_{32} = \sigma_{32}$, $K_{31} = 0$. When setting $V_{23} = 0$ all rates vanish except for K_{12} and K_{21},

$$K_{21} = \frac{\sigma_{21}}{1 + \sigma_{12}\,\tau_a + \sigma_{21}\,\tau_b} \tag{22a}$$

$$K_{12} = \frac{\sigma_{12}}{1 + \sigma_{12}\,\tau_a + \sigma_{21}\,\tau_b} \tag{22b}$$

Eqs.(22) have been derived and analyzed previously.[11] τ_a and τ_b are typical solvent timescales. Eqs.(22) interpolate from the nonadiabatic limit ($\tau_a, \tau_b \to 0$) to the adiabatic limit whereby τ_a and τ_b are long and the rate becomes equal to an inverse solvent timescale. The first term in K_{12}, K_{21}, K_{32} and K_{23} (Eqs.(11a) - (11d)) is an extension of this expression for a three level system. It depends on five different solvent timescales τ_a, τ_b, τ_c, τ'_a, τ'_b. Like Eqs.(22), the first term interpolates between the nonadiabatic rate (for $\tau_j \to 0$) to an inverse average timescale (as $\tau_j \to \infty$). The second term in K_{12}, K_{21}, K_{32}

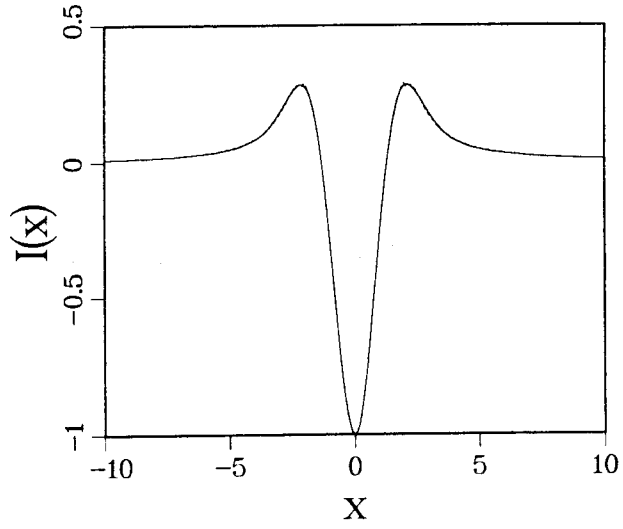

Figure 3: The auxiliary function I(x) (Eq.(19)) (solid line) and its Pade approximant (Eq.(20)) (dashed line).

and K_{23} comes from a coherent process in which the system goes between the states via coherences without passing through a population. A graphical illustration of the terms contributing to K_{21} is given in Figure 2a. All the diagrams lead from population of level 1 (11) to level 2 (22) in fourth order (four bonds). Diagrams (i) - (vi) have a population as an intermediate after two interactions (either 11 or 22). These diagrams contribute to the first term in the expression of K_{21} (Eq.(11a)). Diagrams (vii) and (viii) pass through a coherence (13) after two interactions and they contribute to the second (tunneling) term in Eq.(11a). Similar diagrams can be drawn for K_{12}, K_{32} and K_{23}. K_{31} (Eq.(11e)) has two terms. The first represents the process in which the electron does go through the population of the state |2>, but before it equilibriates with the bath at the state |2>, the electron transfers to state |3>. This term is represented by diagrams (i) and (ii) in Figure 2b. The second term in Eq.(11e) represents the process in which the electron transfers from state |1> to state |3> without actually passing through the state |2>. This is therefore a tunneling process. This term is represented by diagram (iii) in Figure 2b. We shall now consider K_{31} more closely. For simplicity we assume that the relaxation of the system (RC and environment) is sufficiently rapid, $\tau_c \rightarrow 0$, so that the only quantity we need to consider in K_{31} is the second term in Eq.(11e).

We shall now examine a few limiting cases of Eq.(11e). We first consider the case whereby the energy level |2> is sufficiently far from the energy levels |1> and |3>, i.e.

$$\Delta E^1_{12} >> \sqrt{\lambda_{12} k_B T},\ \Delta E^1_{23} >> \sqrt{\lambda_{23} k_B T}. \tag{23}$$

Condition (23) implies that the activation energies $\Delta G^*_{12} \equiv (\Delta G^0_{12} - \lambda_{12})^2/4\lambda_{12}$ and $\Delta G^*_{23} \equiv (\Delta G^0_{23} + \lambda_2 - \lambda_3)^2/4\lambda_{23}$ are much larger than $k_B T$. This limit is where the conventional superexchange theory is usually formulated.[2-4] In this case Eq.(11e) assumes the form

$$K_{31} = \frac{2\pi}{\hbar} |V_{SE}|^2 S_{13}(\Delta E^1_{13}) \tag{24a}$$

with

$$V_{SE} = \frac{V_{12} V_{23}}{\Delta E^1_{12} (\lambda_3/\lambda_{13}) + \Delta E^1_{32} (\lambda_1/\lambda_{13})} . \tag{24b}$$

We next consider another limiting case where all the three states are completely degenerate, i.e. $\Delta E^1_{12} = \Delta E^1_{23} = \Delta E^1_{13} = 0$. We further assume $\lambda_1 = \lambda_2 = \lambda_3 \equiv \lambda$. We then obtain from Eq.(11e)

$$K_{31} = \frac{2\pi}{\hbar} |V_{SE}|^2 S_{13}(0) \tag{25a}$$

where

$$V_{SE} = \frac{V_{12} V_{23}}{\sqrt{3\lambda k_B T}} . \tag{25b}$$

Eqs.(25) may be rationalized using a simple physical argument. The variance of the energy level fluctuations is $\sim \sqrt{\lambda k_B T}$. V_{SE} is thus given by V_{12} V_{23} divided by a typical energy fluctuation.

We have calculated K_{31} using Eq.(11e) and the results are displayed in Figure 4 as a function of $\Delta E^1_{21} = \Delta G^0_{21} + \lambda_{12}$ for different values of ΔE^1_{13}. The dashed line in Figure 4 represents the asymptotic rate expression (Eqs.(24)). Assuming that $K_{32} >> K_{21}$, as suggested by the ultrafast measurements,[5,6] then the sequential rate is equal to K_{21}. The following dimensionless parameter

$$R \equiv \frac{K_{31}}{K_{31} + K_{21}} \tag{26}$$

provides a measure of the relative contribution of the superexchange and the sequential mechanisms. R is bounded between 0 and 1. $R \to 0$ when the sequential transfer dominates, and $R \to 1$ when the superexchange transfer dominates. Figures 5 - 7 display the dependence of R on the energy ΔE^1_{21} for different values of ΔE^1_{13}, coupling V_{12} and reorganization energy λ_{12}.

Our rate expression (Eqs.(11)) was obtained in the high temperature limit. It may be extended to low temperatures by adopting a more specific model for H_B and U_j. A common model in electron transfer theories assumes that U_j is proportional to a single harmonic coordinate representing an intramolecular or intermolecular vibration. In this case Eqs.(11) should be modified by replacing all $k_B T$ factors by the average oscillator energy $\langle \varepsilon \rangle$[6,13]

$$\langle \varepsilon \rangle = \frac{\hbar\omega}{2} \coth \left(\frac{\hbar\omega}{2k_B T}\right) \tag{27}$$

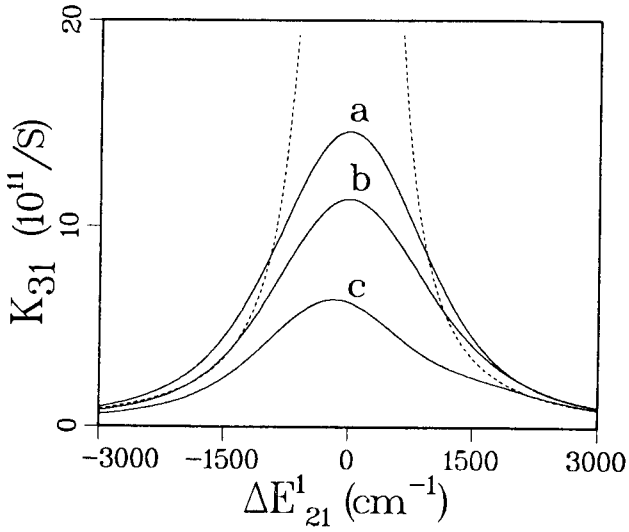

Figure 4: The dependence of the superexchange rate K_{31} on ΔE^1_{21} for different values of ΔE^1_{13}. Curves a, b and c correspond to the ΔE^1_{13} = 0, 400 cm^{-1} and 700 cm^{-1}, respectively. The other parameters in this calculation are: λ_{12} = 1000 cm^{-1}, λ_{23} = 1500 cm^{-1}, λ_{13} = 2000 cm^{-1}, V_{12} = 80 cm^{-1}, $V_{23} = 6V_{12}$, T = 300K. The dashed line represents the conventional superexchange rate (Eqs.(24)) with ΔE^1_{13} = 0.

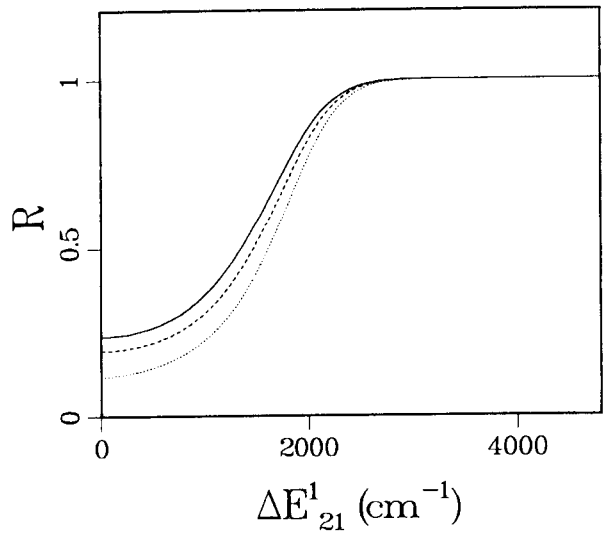

Figure 5: The relative contribution of the superexchange mechanism R is displayed versus ΔE^1_{21} for different values of ΔE^1_{13}. The solid, dashed and dotted lines correspond to ΔE^1_{13} = 0 cm^{-1}, 400 cm^{-1} and 700 cm^{-1}, respectively. The other parameters are: λ_{13} = 2000 cm^{-1}, λ_{23} = 1500 cm^{-1}, λ_{12} = 1000 cm^{-1}, V_{12} = 80 cm^{-1}, $V_{23} = 6V_{12}$, T = 300K.

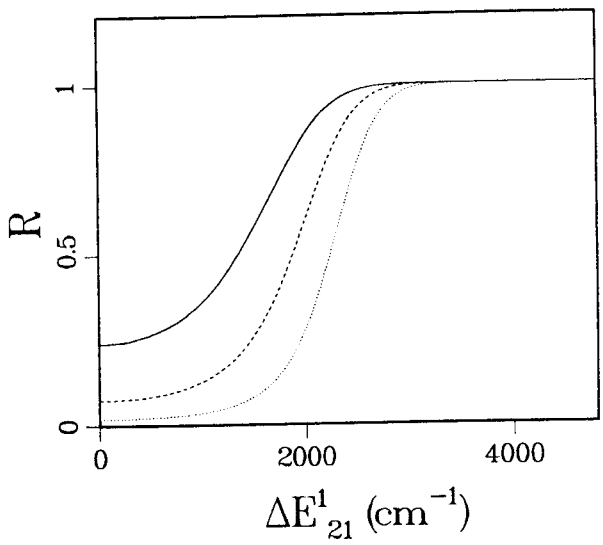

Figure 6: The relative contribution of the superexchange mechanism R is displayed versus ΔE^1_{21} for different values of the coupling V_{12}. These curves correspond to $V_{12} = 80$ cm^{-1} (solid line), 40 cm^{-1} (dashed line) and 20 cm^{-1} (dotted line), respectively. The other parameters are: $\lambda_{13} = 2000$ cm^{-1}, $\lambda_{23} = 1500$ cm^{-1}, $\lambda_{12} = 1000$ cm^{-1}, $\Delta E^1_{13} = 0$, $V_{23} = 6\ V_{12}$, T = 300K.

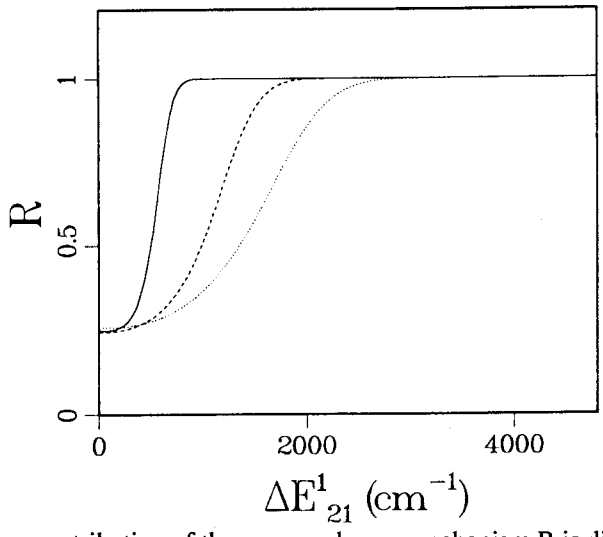

Figure 7: The relative contribution of the superexchange mechanism R is displayed versus ΔE^1_{21} for different values of the reorganization energy λ_{12}. The solid, dashed and dotted lines correspond to $\lambda_{12} = 100$ cm^{-1}, 500 cm^{-1} and 1000 cm^{-1}, respectively. The other parameters are: $\Delta E^1_{13} = 0$, $\lambda_{13} = 2000$ cm^{-1}, $\lambda_{23} = 2000$ cm^{-1}, $V_{12} = 80$ cm^{-1}, $V_{23} = 6\ V_{12}$, T = 300K.

Note that in the high temperature ($k_BT>>\hbar\omega$) limit $<\varepsilon> = k_BT$. When k_BT in Eqs.(11) is replaced by $<\varepsilon>$ (Eq.(27)) we obtain a rate expression which is not restricted to the high temperature limit. Martin, et.al.[6] have measured the temperature dependence of the RC electron transfer in the range 10K to 300K. For Rb. sphaeroides the variation of the rate was found to be in agreement with the conventional superexchange rate (Eqs.(24)) assuming a single mode with ω=80 cm^{-1}. For Rps. viridis on the other hand the conventional expression is inadequate and the best fit obtained[6] (using ω=25 cm^{-1}) is shown in Figure 8 (dashed line). The temperature dependence predicted by our present theory for K_{31} (Eq.(11e) together with Eq.(27)) is found to be in a much better agreement with experiment. This is illustrated in Figure 8.

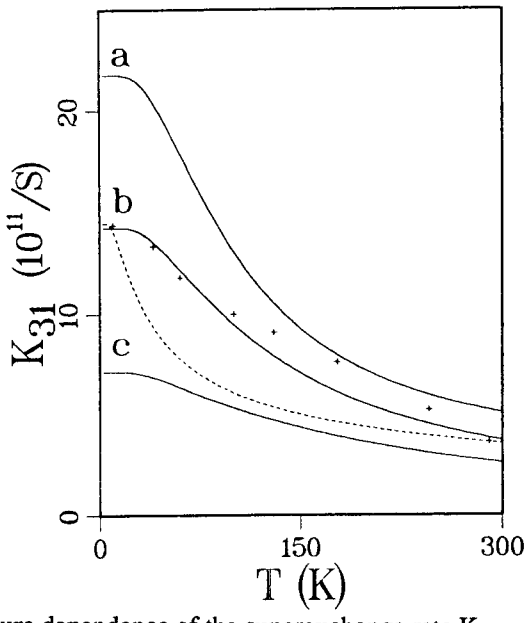

Figure 8: Temperature dependence of the superexchange rate K_{31}. A coupling to a single vibrational mode with ω=90 cm^{-1} is assumed and the calculation was made using Eq.(11e) with k_BT replaced by $<\varepsilon>$ (Eq.(27)). Curves a, b and c correspond to ΔE^1_{21} = 800 cm^{-1}, ΔE^1_{21} = 1050 cm^{-1} and ΔE^1_{21} = 1500 cm^{-1}, respectively. The dashed curve represents the best fit with the conventional superexchange rate using ω = 25 cm^{-1} (Eq.(2) in Reference 6). The points (+) denote the experimental results of electron transfer rate in Rps. viridis from Martin, et.al.[6] Other parameters in this calculation are λ_{13} = 2000 cm^{-1}, λ_{12} = 200 cm^{-1}, λ_{23} = 2000 cm^{-1}, V_{12} = 79 cm^{-1}, V_{23} = 6 V_{12}, ΔE_{13} = 0. This figure shows that our superexchange expression (curve b) provides a better fit with experiment, compared with the conventional superexchange expression (dashed line).

Acknowledgement

The support of the Office of Naval Research, the National Science Foundation and the Petroleum Research Fund, administered by the American Chemical Society, is gratefully acknowledged.

References

1. See papers in "The Photosynthetic Bacterial Reaction Center" edited by Jacques Breton and Andre Vermeglio, Plenum, NY (1988).

2. R.A. Marcus, Chem. Phys. Letters **133**, 471 (1987); in Reference 1, p.389.

3. M. Bixon, J. Jortner, M. Plato and M.E. Michel-Beyerle in Reference 1, p.399.

4. A. Beretan and J.J. Hopfield, Journ. Am. Chem. Soc. **106**, 1584 (1984); M. Redi and J.J. Hopfield, J. Chem. Phys. **72**, 6651 (1980); J.R. Miller and J.V. Beitz, J. Chem. Phys. **74**, 6746 (1981).

5. J. Breton, J.L. Martin, A. Migus, A. Antonetti and A. Orszag, Proc. Nat. Acad. Sci. USA **83**, 5121 (1986); G.R. Fleming, J.L. Martin and J. Breton, Nature **333**, 190 (1988).

6. J.L. Martin, J. Breton, J.C. Lambry and G.R. Fleming in Reference 1, p. 195.

7. J.M. Hayes and G.S. Small, J. Phys. Chem. **90**, 4928 (1986); S.R. Meech, A.J. Hoff and D.A. Wiersma, Chem. Phys. Lett. **121**, 287 (1985); S.J. Boxer, D.S. Gottfried, D.J. Lockhart and T.R. Midderdorf, J. Chem. Phys. **86**, 2439 (1987).

8. Y. Won and R.A. Friesner, J. Phys. Chem. **92**, 2214 (1988).

9. Y. Won and R.A. Friesner, Biochem. Biophys. Acta **935**, 9 (1988).

10. Y. Hu and S. Mukamel (to be published).

11. M. Sparpaglione and S. Mukamel, J. Chem. Phys. **88**, 5 (1988); Y.J. Yan, M. Sparpaglione and S. Mukamel, J. Phys. Chem. **92**, 4842 (1988).

12. S. Mukamel, Adv. Chem. Phys. **70**, 165 (1988).

13. M. Bixon and J. Jortner, J. Phys. Chem. **90**, 3795 (1986).

14. J.S. Bader and D. Chandler, Chem. Phys. Lett. (in press).